The Effect of Three Different 4-Hydroxy-1,3,3a,7-tetraazaindenes on the Melt pAg, Ionic Activation Energies and Photocarrier Responses of an AgBr Emulsion

Lillian M. Kellogg
Eastman Kodak Company, Imaging Research and Advanced Development
Rochester, New York

Abstract

Melts and coatings of a 0.3 μm octahedral AgBr emulsion were prepared with 4 concentrations of each of 3 different 4-hyroxy-1,3,3a,7-tetraazaindene molecules (TAIs). pAg measurements were made on the melt samples and ionic thermocurrent (ITC) and radiofrequency photoconductivity (RF) measurements were made on the coated samples. The melt pAg (i.e., the Br^- desorbed from the grain surface) increased as the pK_{sp} and the concentration of the TAI in the sample increased. The concentration of desorbed Br^- measured as a function of TAI concentration was consistent with the proposal that TAI anions (TAI^-) compete with Br^- for adsorption to the surface of the grain. The ionic activation energy for formation of interstitial silver ions and the photoelectron lifetime increased as the pK_{sp} and the concentration of TAI^- increased. A linear correlation between desorbed Br^- and ionic activation energy was observed. The presence of TAI did not affect the photohole response. For TAIs with $pK_a < 5.0$, these effects were independent of pH for pH values between 4.5 and 7.0, whereas when $pK_a > 6$, these effects decreased with decreasing pH.

Introduction

It has been reported in the literature[1] that 4-hydroxy-6-methyl-1,3,3a,7-tetraazaindene (6-Me TAI)

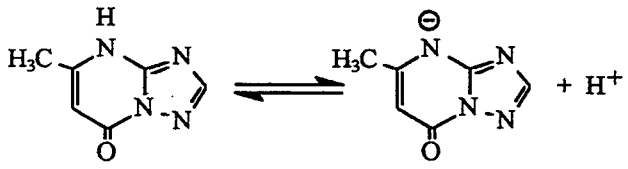

is a weak acid that:

1. Only adsorbs to the silver halide grain in its anionic form.
2. As an anion competes with the excess Br^- in the melt for adsorption to the grain surface.

This proposed competition for the surface is shown below in Eqn. (1).

$$TAI^-_{(solution)} + Br^-_{(adsorbed)} \leftrightarrow TAI^-_{(adsorbed)} + Br^-_{(solution)} \quad (1)$$

If this model is correct the concentration of Br^- in the solution should increase as the concentration of TAI^- adsorbed to the grain increases and this should only occur when the solution pH is high enough for the TAI molecules to be ionized.

To test this model, pAg measurements were made on emulsion melts as a function of TAI concentration and melt pH for three TAI molecules. These molecules and their pK_a and pK_{sp} values are defined in Table 1 according to the following general structure.

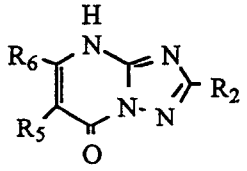

Table 1

Compound I.D.	R_2, R_5, R_6	40°C pK_a	40°C pK_{sp}
6-Me TAI	H, H, Me	6.18	10.98
5-Br TAI	H, Br, Me	4.79	12.17
6-MeSOMe TAI	H, H, MeSOMe	4.35	9.42

The pK_{sp} values listed in Table 1 show the negative log of the solubility product of the 1 to 1 TAI^- - silver salt. These values were measured in solution using a solid-state silver sulfide electrode.[2]

Experimental - pAg Studies

The TAI^- levels used in these experiments for all three of the TAI compounds were 1.16, 2.32, 5.8, and 11.8 mmol/Ag mol. To detect Br^- desorption from the surface of the 0.3 μm AgBr octahedral emulsion used in this study, the emulsion melts were adjusted to pH 7.0 and pAg 8.33, and pAg measurements were made both before and after the TAI^- additions using a standard Ag/AgBr electrode.

In these experiments the solution pAg was observed to increase as the concentration of TAI^- increased indicating that the concentration of Br^- in solution increased with the addition of TAI^- as predicted by Eqn.(1).

In order to compare the effects that these 3 TAI anions have on the emulsion grain it is helpful to plot mmol of $Br^-_{(desorbed)}$/Ag mol as a function of the concentration of added TAI^-, where $[Br^-]_{desorbed} = [Br^-]_{solution(after\ TAI\ addition)} - [Br^-]_{solution(before\ TAI\ addition)}$. This plot is shown in Figure 1.

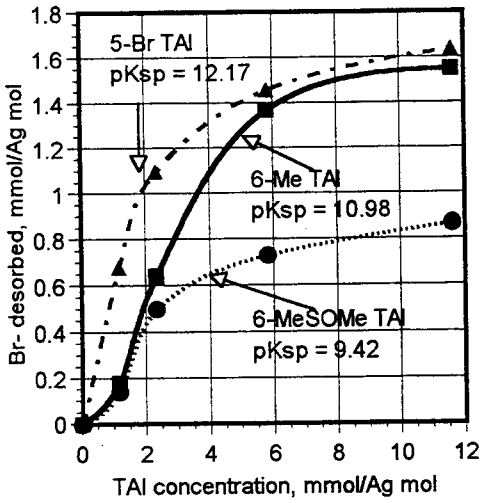

Figure 1. Plot of the concentration of desorbed Br^- in mmol/ Ag mol versus concentration of TAI added.

This plot shows that the amount of Br^- that is desorbed from the surface of the AgBr grain is dependent on the concentration and pK_{sp} of the TAI molecule as would be expected if Eqn. (1) is valid. The maximum level of desorbed Br^- measured in these studies is very close to the maximum level of excess Br^- present on the grain as determined in reference 1.

To test the proposal that the deprotonated form of the TAI molecule is the photographically active form, 5.8 mmol of each of the three TAI compounds were added to separate emulsion melts that were adjusted to pAg 8.33 and pH 4.5. The pAg of each melt was then measured as the melt pH was increased stepwise from 4.5 to 7.0. A plot of melt pAg versus melt pH after TAI addition is shown in Figure 2.

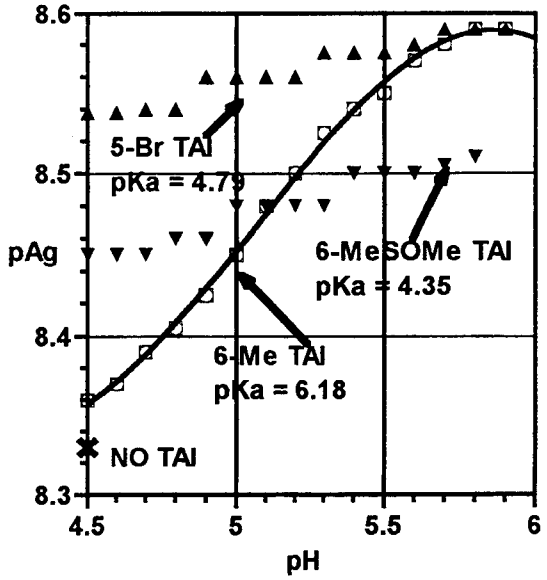

Figure 2. Plot of melt pAg versus melt pH after TAI^- addition.

This figure shows that addition of the 5-Br TAI^- or the 6-MeSOMe TAI^- at pH 4.5 resulted in an increase in pAg with very little additional increase in pAg with increasing pH. For 6-Me TAI, there was very little increase in pAg when this compound was added at pH 4.5, but the pAg of the melt increased as the pH of the melt increased. This result is consistent with the proposal that the deprotonated form is the photographically active form, since 5-Br TAI and 6-MeSOMe TAI would be substantially deprotonated at pH 4.5, whereas the 6-Me TAI with a pK_a of 6.18 would not. The 6-Me TAI does deprotonate as the pH increases and, therefore, does desorb Br^- at the higher pH values.

All the solution data, are consistent with the proposal in reference (1) that TAI anions compete with Br^- for adsorption to the surface of the grain. This interaction, then, should be described by Eqn. (1) which can be rearranged to give Eqn. (2).

$$TAI^-_{solution} + Br^-_{adsorbed} \leftrightarrow TAI^-_{adsorbed} + Br^-_{solution} \quad (1)$$

$$K_{eq} = \frac{[TAI^-_{ads.}]\,[Br^-_{soln.}]}{[TAI^-_{soln.}]\,[Br^-_{ads.}]} \quad (2)$$

This equilibrium expression can be evaluated by assuming that:

1. $[TAI^-_{ads.}] = [Br^-_{desorbed}]$ and
2. $[Br^-_{ads.}]_{initial}$ is known, i.e. the value reported in ref. 1 as maximum Br^- coverage/unit surface area for an octahedral AgBr emulsion.
3. $[Br^-_{ads.}] = [Br^-_{ads.}]_{initial} - [Br_{desorbed}]_{measured}$
4. $[Br^-_{soln.}] = [Br^-]_{measured}$
5. $[TAI^-_{soln.}] = [TAI^-]_{added} - [TAI^-_{ads.}]$.

Since all these quantities are known or measured, K_{eq} can be evaluated for the different TAI anions. The results of these evaluations are shown in Table 2.

Table 2

Compound	pK_{sp}	K_{eq}
5-Br TAI	12.17	4.96
6-Me TAI	10.98	1.00
6-MeSOMe TAI	9.42	0.48

Once K_{eq} is evaluated it can be used to calculate adsorbed TAI$^-$ (desorbed Br$^-$) at any TAI$^-$ concentration. The results of these calculations are shown in Figure 3 for 5-Br TAI$^-$.

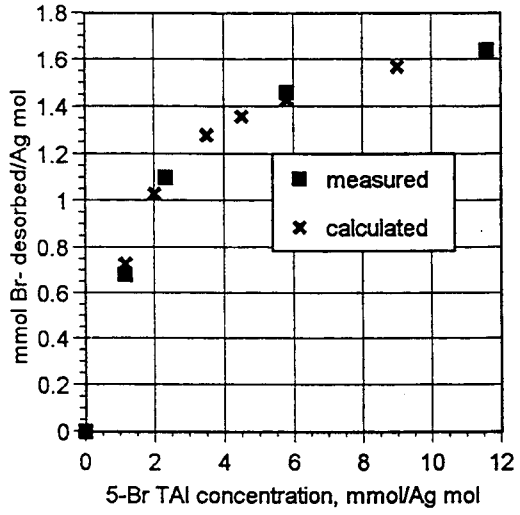

Figure 3. Plot of mmol of Br$^-$ desorbed versus mmol of 5-Br TAI$^-$ added for both measured and calculated values.

This plot shows that there is good agreement between the measured and calculated values of desorbed Br$^-$ using these assumptions.

Ionic Thermocurrent Measurements

It is well known that the adsorption of 6-Me TAI to the surface of a silver bromide grain results in a decrease in the ionic conductivity[3, 4] and that the ionic conductivity decreases as the concentration of Br$^-$ in the emulsion melt decreases.[5, 6] In addition, grains that have higher levels of excess surface halide have higher concentrations of interstitial silver ions, i.e., at the same pAg, octahedral grains will have a higher ionic conductivity than cubic grains.[7] These results have led to the assumption that the interstitial silver ions in silver bromide grains are compensated by the excess Br$^-$ at the surface of the grain. The question of what happens to the ionic conductivity as a larger, more diffuse, TAI anion replaces a surface bromide ion is, therefore, of some interest.

For the ionic thermocurrent (ITC) measurements[8] all of the samples of the concentration series and 3 of the pH adjusted samples were coated on a strippable base at a silver coverage of 38.7 g/m^2 Ag and 43.0 g/m^2 gelatin. For these measurements the coated sample was removed from the film base and placed between two electrodes in a cryogenic refrigerator. A field was placed across the sample, it was cooled to 10 K and the field was removed. The sample was then heated at a linear rate. When the temperature was high enough for the interstitial ions to relax the imposed field a current was observed in the external circuit. The temperature of the current peak provides a measure of the ionic activation energy. The calibration curve used to relate peak temperatures to activation energies was originally determined by comparison with activation energies measured using the dielectric loss technique.

Figure 4, a plot of current in picoamps versus absolute temperature, shows the ITC spectra for the control emulsion and for the 5-Br TAI concentration series.

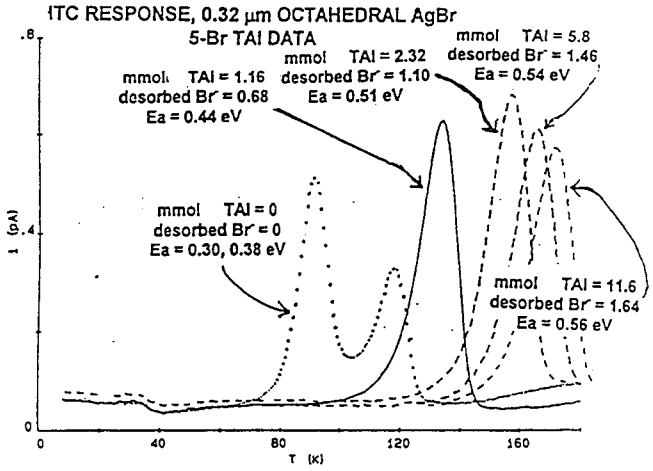

Figure 4. Plot of signal in picoamps versus absolute temperature for the 5-Br TAI concentration series.

Figure 4 shows that the temperature required for the interstitial silver ions to move to relax the external field in these grains increases as the concentration of 5-Br TAI$^-$ increases. The ionic activation energies, E_a, associated with the measured peaks are also shown in Figure 4. The higher the ionic activation energy the lower the concentration of interstitial silver ions. So as the concentration of 5-Br TAI$^-$ adsorbed to the emulsion grain increases, the concentration of interstitial silver decreases.

Table 3 lists the ionic activation energies, E_a, measured for the samples coated at a concentration of 5.8 mmol/Ag mol for each of the TAI compounds.

Table 3

Compound	pK_{sp}	E_a (eV)
NONE		0.30, 0.38
5-Br TAI	12.17	0.54
6-Me TAI	10.98	0.53
6-MeSOMe TAI	9.42	0.47

This table shows that the shift in the ionic activation energy with TAI addition increases as the pK_{sp} of the TAI compound increases.

The relation between surface charge and ionic activation energy was derived by R. Poeppel and J. Blakely[9] to be,

$$e\phi_s = 0.67 - E_a \qquad (3)$$

where $e\phi_s$ = the surface charge, and
0.67 = the energy to form an interstitial vacancy pair in the silver halide lattice.

If it is assumed that the surface charge is provided by the excess anions at the surface of the grain, and the ionic activation energy increases as the TAI anions replace the Br anions, then if Eqn. (3) is valid, the charge density for a TAI anion must be different than that of a bromide ion. If this is the mechanism for the increase in the ionic activation energy, the ionic activation energy should be dependent on the concentration of Br^- adsorbed to the grain, or conversely on the concentration of TAI^- adsorbed to the grain. Assuming that

$$[TAI^-_{adsorbed}] = [Br^-_{desorbed}] \text{ and}$$
$$[Br^-_{adsorbed}] = [Br^-_{adsorbed}]_{initial} - [Br^-_{desorbed}]_{measured}$$

then the ionic activation energy can be plotted versus $[TAI^-_{adsorbed}]$ shown in Figure 5, or $[Br^-_{adsorbed}]$ shown in Figure 6.

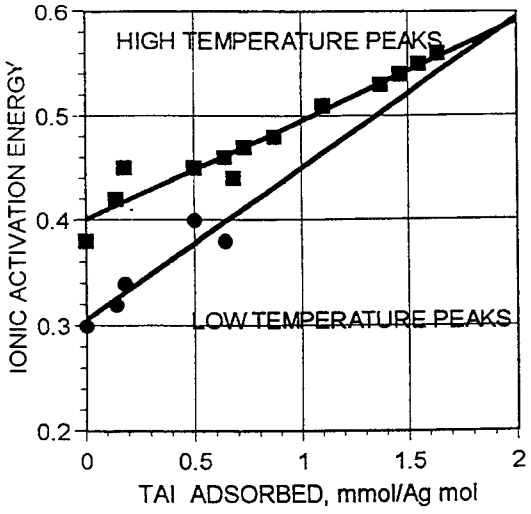

Figure 5. Plot of mmol of adsorbed TAI^- versus measured ionic activation energy.

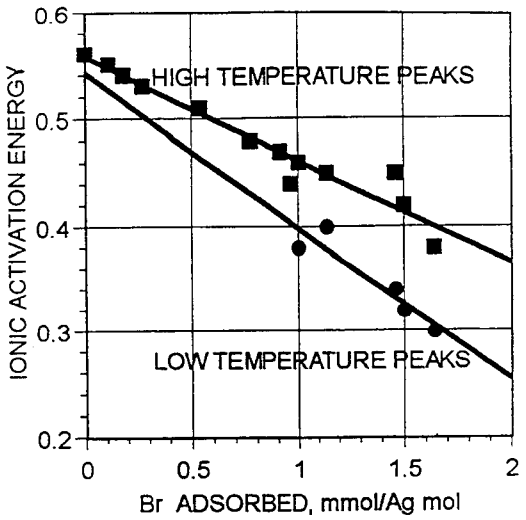

Figure 6. Plot of mmol of adsorbed Br^- versus measured ionic activation energy.

Figure 5 shows that the ionic activation energy increases as the concentration of TAI^- adsorbed to the surface of the grain increases. Conversely, Figure 6 shows that the ionic activation energy decreases as the concentration of Br^- adsorbed to the surface of the grain increases. These plots also show a linear relation between adsorbed surface anions and the activation energy. These results are consistent with the assumption that the adsorbed anions control the surface potential.

Radiofrequency Photoconductivity Measurements

For the radiofrequency (RF) photoconductivity measurements, all the melt samples were coated on a subbed base at a silver coverage of 4.3 g/m^2 and a gelatin coverage of 4.8 g/m^2. In these measurements the film sample was placed in a sample capacitor. A variable capacitor and the RF frequency were adjusted to balance the RF bridge. The sample was then exposed and the decay curves were recorded as the carriers were trapped and the bridge was rebalanced. With this, apparatus both electron and hole responses can be detected at room temperature.[10]

Because the (RF) photoconductivity technique can detect both photohole and photoelectron responses, it is necessary to characterize differences in the two responses. To do this, the photoconductivity response, plotted as signal in mV versus time in microseconds, of a reference sample coated with an electron trapping dye was measured and plotted in Figure 7a, and the photoconductivity response of the sample coated with a hole trapping dye was measured and plotted in Figure 7b. Neither sample was chemically sensitized.

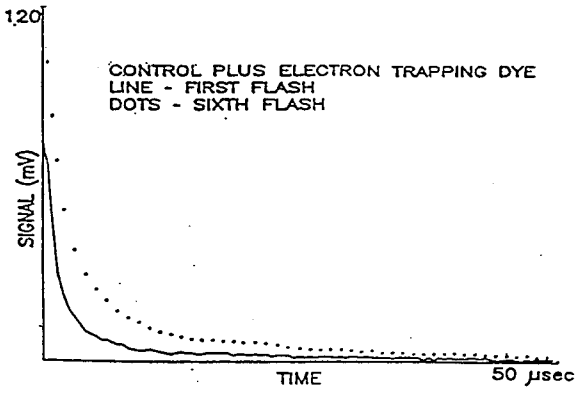

Figure 7a. Room temperature photohole response for a reference emulsion.

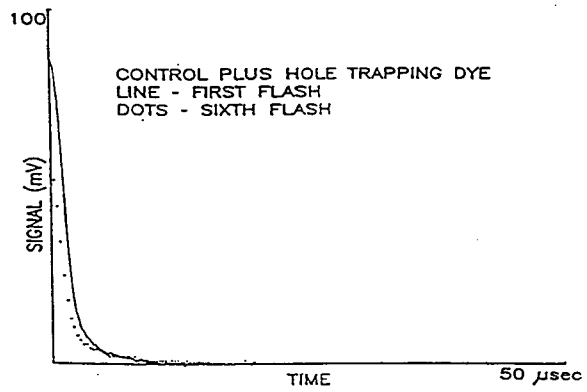

Figure 7b. Room-temperature photoelectron response for the reference emulsion.

Since, for the sample in Figure 7a all the photoelectrons are trapped, this plot shows the room-temperature photohole response, which is a relatively long, low magnitude signal that increases on exposure. The room-temperature photoelectron response, shown in Figure 7b, is a shorter, higher response that decreases on exposure.

The room-temperature photoconductivity response for the sample prepared with 2.32 mmol/Ag mol of 6-Me TAI is shown in Figure 8.

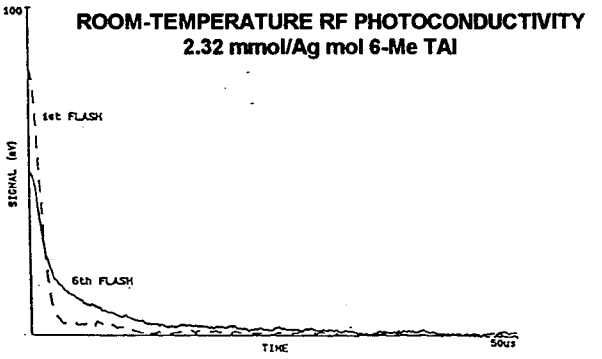

Figure 8. Photoresponse for sample coated with 6-Me TAI⁻.

Figure 8 shows a two-component decay curve comprised of a short component that decreases on exposure and a long component that increases on exposure. This result implies that 6-Me TAI⁻ is not acting as either an electron trap or a hole trap, since both electron and hole responses are observed for this sample and at mmolar levels any electron or hole trapping compound should trap all the carriers generated in these exposures.

Even though the TAI anions studied do not act as electron or hole traps, it is well known that the addition of 6-Me TAI⁻ to an octahedral emulsion increases the photoelectron lifetime.[11] In order to study this effect and measure actual lifetimes for all of the TAI levels, the photoelectron lifetimes were measured at -140°C, where the electron is the dominate carrier. Table 4 shows the change in the photoelectron lifetime with increasing 5-Br TAI⁻ concentration.

TABLE 4

5-Br TAI Concentration mmol/Ag mol	PHOTOELECTRON Lifetime, @ -140°C microseconds
0	5.7, 0.97
1.16	44
2.32	270
5.80	630
11.60	910

This table shows that the photoelectron lifetime increases as the concentration of 5-Br TAI increases.

Since the days of Gurney and Mott[12] it has been assumed that interstitial silver ions are somehow involved in the trapping of the photoelectrons. Although specific mechanisms[12-14] are different in details, most would predict that at constant temperature, the rate of electron trapping, $k_t = 1/\tau$, where τ is the measured photoelectron lifetime, should be proportional to the interstitial silver ion concentration. If this is true,

$$k_t \propto [Ag_i^+] \quad \text{and} \tag{4}$$

$$\ln k_t \propto -E_a/kT + \text{constant} \tag{5}$$

To test whether the increases in photoelectron lifetime (observed when the TAI anions were added to the emulsion grain) were due to a decrease in the interstitial silver ion concentration, ln k_t was plotted versus the measured ionic activation energy for all the samples studied. This plot is shown in Figure 9.

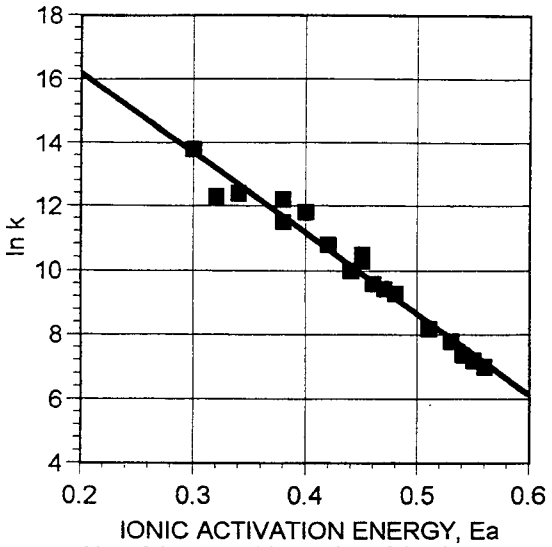

Figure 9. Plot of the natural logarithm of the electron trapping rate, k_t, versus the ionic activation energy.

This plot shows that there is a linear relation between ln k_t and the ionic activation energy and that the electron trapping rate decreases as the ionic activation energy increases. This implies that the decrease in electron trapping rate observed with the addition of the TAI anions is due to the decrease in the interstitial silver ion concentration and not to a direct interaction between the TAI anions and the photoelectrons.

Summary of Physical Measurement Results

All the results presented in this study are consistent with the model proposed by Shiao et al,[1] that states that TAI anions compete with the excess surface Br^- for adsorption to the grain, and that the adsorption of TAI^- results in the desorption of the excess surface Br ions. This desorption of Br^- results in a decrease in the excess negative charge on the surface of the grain and an increase in the ionic activation energy. As the ionic activation energy increases the interstitial silver ion concentration decreases and the concentration of electron traps decreases. None of the TAI anions studied acted as electron traps or as hole traps. There was also no evidence that the TAI anions replaced lattice bromide ions, i.e., the maximum concentration of Br^- desorbed from the grain was equal to the concentration of excess Br^- adsorbed to the grain.

References

1. D. D. F. Shiao, M. T. Nieh and A. H. Herz, *J. Photogr. Sci.*, **30**, 208 (1982).
2. R. Klaus, Private Communication.
3. J. Van Biesen, *J. Appl. Phys.*, **41**(5), 1910 (1970).
4. T. Takada, *Photogr. Sci. Eng.*, **18**, 500 (1974).

4b. H. A. Hoyen Jr., *J Appl. Phys.*, **47**, 3784 (1976).

5. F. Callens, W. Maenhout-van der Vorst, L. Ketellaper, *Phys. Status Solidi (a)*, **70**, 189 (1982).
6. F. P. Chen, K. C. Chang, L. Corben, M. Falxa, B. Levy, *Photogr. Sci. Eng.*, **26(1)**, 15 (1982).
7. K. Ohzeki, S. Urabe, T. Tani, J. *Imaging Sci.* **34**, 136 (1990).
8. A. R. Valla, J. M. Hodes, *Photogr. Sci. Eng.* **25**, 240 (1981).
9. R. Poeppel, J. Blakely, *Surface Sci.*, **15**, 507 (1969)
10. L. M. Kellogg, J. M. Hodes, Proceedings of SPSE East-West Meeting, Kona, Hawaii (1988).
11. T. Tani, *Photogr. Sci. Eng.* **21**, 37 (1977).
12. N. F. Mott, R. W. Gurney, "Electronic Processes in Ionic Crystals", Dover Publications, NY, 1948, p228.

13a. B. E. Bayer and J. F. Hamilton, *J. Opt. Soc. Am.*, **55**, 439 (1965).

13b. J. F. Hamilton and B. E. Bayer, *J. Opt. Soc. Am.*, **55**, 528 (1965).

14a. W. F. Berg and K. Mendelssohn, *Proc. R. Soc. Lond.*, **A168**, 168 (1938).

14b. J. W. Mitchell, Rep. *Progr. Phys.* **20**, 433 (1957).